Analyst

PAPER

View Article Online
View Journal | View Issue

Cite this: *Analyst*, 2015, **140**, 3210

MoS_2 nanosheets as an effective fluorescence quencher for DNA methyltransferase activity detection†

Huimin Deng, Xinjian Yang and Zhiqiang Gao*

Received 20th November 2014,
Accepted 2nd March 2015

DOI: 10.1039/c4an02133a

www.rsc.org/analyst

As one of the inorganic graphene analogues, two dimensional MoS_2 nanosheets have been drawing extensive attention in the past few years due to their remarkable structural and electronic properties. Herein, a simple signal-on fluorescence DNA methyltransferase (MTase) activity assay using a MoS_2 nanosheet mediated fluorescence quenching strategy is described. Briefly, substrate DNA is designed to possess a double-stranded DNA (ds-DNA) segment containing the recognition sequence of DNA adenosine methyltransferase (Dam) and a single-stranded DNA (ss-DNA) segment for anchoring the substrate DNA to MoS_2 nanosheets *via* van der Waals interactions. Once the substrate DNA is absorbed onto MoS_2 nanosheets, the fluorescence of the fluorophores labeled to the end of the ds-DNA region is quenched. When the substrate DNA is methylated by Dam, fluorescence is recovered resulting from the release of the fluorophore labeled segment cleaved by the methylation sensitive restriction endonuclease DpnI. Since the fluorescence recovery directly reflects the methylation level, the Dam MTase activity can be quantified accordingly. Based on this assay, a linear range of 0.2–20 U mL^{-1} is achieved with high sensitivity and selectivity. Furthermore, the inhibitor screening ability is well demonstrated.

Introduction

DNA methyltransferases (MTases) are a family of enzymes that catalyze the transfer of a methyl group from *S*-adenosyl-L-methionine (SAM) to adenine or cytosine residues in the specific site of DNA during the biological DNA methylation process.[1] DNA methylation is one of the most commonly occurring epigenetic events that plays essential roles in the regulation of gene expression.[2–5] In mammals, abnormal DNA methylation patterns caused by altered DNA MTase activity have been demonstrated to be closely associated with several types of cancer, such as gastric cancer and lung cancer.[6,7] Consequently, DNA MTases have been recognized as potential targets for early disease diagnosis. Therefore, the development of DNA MTase activity assays is critical for both scientific research and clinical application.

Traditional DNA methylation and MTase activity analysis methods mainly include the use of ^3H NMR, methylation-specific polymerase chain reaction (PCR)-based techniques, gel electrophoresis, and high performance liquid chromatography/mass spectrometry.[8–11] Such methods have the drawbacks of time-consuming, requirement of radio-labeled substrate or sophisticated equipment. Recently, novel DNA MTase activity assays, which are relatively simple, time-saving, or cost effective, have been developed based on different sensing techniques, such as fluorometry,[12,13] colorimetry,[14,15] and electrochemistry.[16,17] Benefited from the rapid development of nanoscience, lots of nanomaterials have been employed in the abovementioned DNA MTase assays to act as either signal producers or signal amplifiers. For example, Ouyang and coworkers have reported a low-background Dam MTase activity fluorescence sensing platform using carboxylated carbon nanoparticles as a fluorescence quencher coupled with a DNA intercalator dye.[18] Liu *et al.* have also established a sensitive Dam MTase activity assay based on the methylation/cleavage reaction induced aggregation of duplex substrate DNA modified gold nanoparticles.[15] In addition, based on the signal transduction and amplification of single wall carbon nanotubes, a label-free electrochemical approach for the detection of MTase activity has been confirmed by Wang and collaborators.[19]

As a conceptually new class of nanomaterials, two-dimensional (2D) inorganic graphene analogues (IGAs) have been considered to be an emerging area in nanoscience.[20,21] Due to the unique electronic properties that are driven from their ultrathin structure, IGAs such as layered transition metal dichalcogenides (TMDCs, *e.g.*, MoS_2 and WS_2) and boron

Department of Chemistry, National University of Singapore, 3 Science Drive 3, Singapore 117543. E-mail: chmgaoz @nus.edu.sg; Fax: +65-6779-1691; Tel: +65-6516-3887

†Electronic supplementary information (ESI) available. See DOI: 10.1039/c4an02133a

nitride have drawn intensive attention in the past few years and have shown various potential applications in catalysis, energy storage, and sensing.[22–24] Up to now, the biosensing applications of IGAs are relatively rare and are yet to be fully discovered. In 2013, Zhang's group reported the usage of single-layered MoS_2 for homogeneous detection of DNA and adenosine for the first time.[25] Much more recently, based on the fact that 2D TMDCs preferentially absorb single-stranded oligonucleotides toward double-stranded ones, similar approaches were developed for DNA and microRNA sensing by using WS_2 nanosheets.[26,27] Moreover, some other biological sensing systems involving layered MoS_2 nanomaterials have been investigated for the detection of glucose, cancer biomarkers, and hydrogen peroxide.[28–30]

Motivated by the abovementioned biological sensing studies based on the newly emerging 2D layered IGAs, we explored the application of MoS_2 nanosheets in the MTase activity assay. In this work, a signal-on fluorescence Dam MTase activity assay employing MoS_2 nanosheets as a fluorescence quencher was successfully demonstrated. Its simplicity, rapidity, low cost in conjunction with high sensitivity and selectivity make it attractive as a candidate for MTase activity analysis.

Experimental

Materials and apparatus

Molybdenum(IV) sulphide and 5-fluorouracil were purchased from Sigma-Aldrich (St Louis, MO, USA). Tris(hydroxymethyl)-aminoethane (Tris) was obtained from Alfa Aesar (Lancashire, England). Dam MTase, AluI MTase, M.SssI MTase, DpnI endonuclease, and *S*-adenosyl-L-methionine (SAM) were purchased from New England Biolabs (Ipswich, MA). The Dam methylation and DpnI cleavage reactions were performed in a reaction buffer (R buffer: 20 mM Tris-HAc, 50 mM KAc, 10 mM $Mg(Ac)_2$, 100 μg mL^{-1} BSA, pH 7.9). Oligonucleotides used in this work were custom-made by 1st Base Pte Ltd (Singapore). The sequences of the oligonucleotides were as following: oligonucleotide 1 (oligo 1): 5′-CCT GGA GTT GAT CAT ATC TGG ACC TAT AGT TCA CTT-3′ and the FAM dye labeled partially complementary oligonucleotide 2 (oligo 2): 5′-FAM-TAT GAT CAA CTC CAG G-3′. The two oligonucleotides were dissolved in TE buffer (10 mM Tris, 1 mM EDTA, pH 8.0) to the desired concentrations and stored at −20 °C. All other chemicals of certified analytical grade were used without further purification. All aqueous solutions were prepared with ultrapure water (18.3 MΩ).

Atomic force microscopy (AFM) image of layered MoS_2 was acquired with a tapping mode on a Veeco Digital Instruments Dimension 3000 SPM. The UV-vis absorption spectrum was recorded on an Agilent Cary 60 UV-vis spectrophotometer. Fluorescence was recorded on an Agilent Cary Eclipse fluorescence spectrophotometer.

Preparation of MoS_2 nanosheets

The MoS_2 nanosheets were prepared according to a reported mixed-solvent exfoliation procedure with some modifications.[31] Briefly, 150 mg MoS_2 powder was added to a 100 mL flask, 50 mL ethanol–water (45%, v/v) was added as the dispersion solvent. The mixture was sonicated for 8 h, and then the dispersion was centrifuged at 5000 rpm for 30 min to remove aggregates. The supernatant was collected and the concentration of the MoS_2 nanosheet dispersion was measured by using an UV-vis spectrophotometer.

Feasibility study

A double-stranded substrate DNA was prepared by mixing equal moles of oligo 1 and oligo 2 in a hybridization buffer (10 mM Tris-HCl, 100 mM NaCl, pH 7.4), the mixture was heated to 90 °C for 5 min, then slowly cooled down to room temperature, and stored at 4 °C if not in use. To investigate the activities of Dam and DpnI in the same R buffer and avoid the change of buffers for different enzymatic reactions, different ds-DNA samples were prepared by treating 4 μM ds-DNA with 16 units of Dam, 20 units of DpnI, and 16 units of Dam + 20 units of DpnI in R buffer containing 160 μM SAM respectively. Both the methylation and cleavage reactions were performed at 37 °C for 2 h. Then, the DNA samples were characterized by 15% polyacrylamide gel electrophoresis.

On the other hand, to evaluate the fluorescence quenching and recovery mediated by the MoS_2 nanosheets, 50 μL 100 nM ds-DNA and 50 μL 100 nM Dam/DpnI pre-treated ds-DNA in R buffer were mixed with 50 μL as-prepared MoS_2 nanosheets respectively. The mixture was allowed to stand for 15 min, and then centrifuged at 6000 rpm for 1 min to minimize the background signal. Finally, the supernatant was collected by using a pipette for fluorescence measurement with an excitation wavelength of 495 nm.

Dam methyltransferase activity assay

The enzymatic reactions were conducted in a 200 μL total reaction volume. The typical reaction mixture consisted of 100 nM ds-DNA, 160 μM SAM, and various concentrations of Dam MTase in R buffer. The mixture was first incubated at 37 °C for 2 h, then 0.5 μL of 20 000 U mL^{-1} DpnI was added and further incubated for another 2 h. After the reaction, 50 μL of the mixture was mixed with 50 μL of the as-prepared MoS_2 nanosheets for 10 min at room temperature, followed by centrifugation at 6000 rpm for 1 min. The fluorescence intensity of the supernatant was recorded finally.

Selectivity and inhibition study

The selectivity of the proposed Dam activity assay was evaluated by using two other kinds of MTases. The procedure was the same as the above described Dam activity detection procedure, except that Dam was replaced by AluI and M.SssI respectively. The concentration of MTase was 20 U mL^{-1} for each. Similarly, the inhibition study was carried out by the same procedure with 20 U mL^{-1} Dam MTase, and different concentrations of 5-fluorouracil were added together with Dam in the methylation process. Control experiments were also performed without the addition of Dam MTase in both the

selectivity and inhibition studies. The relative activity of Dam MTase inhibited was calculated as follows:

$$\text{Relative activity } (\%) = \frac{F_2 - F_0}{F_1 - F_0} \times 100\%$$

where F_0 is the fluorescence intensity of 0 U mL^{-1} Dam MTase, F_1 is the fluorescence intensity of 20 U mL^{-1} Dam MTase and F_2 is the fluorescence intensity after the inhibitor treatment.

Results and discussion

Characterization of MoS_2 nanosheets

The MoS_2 nanosheets were prepared by a simple sonication assisted ethanol–water mixed solvent exfoliation method from bulk MoS_2 powder. The obtained dark-green suspension (Fig. 1, inset) was highly stable, and showed no precipitation after being stored for several weeks under ambient conditions. Fig. 1 shows the UV-vis spectrum of the suspension which agrees well with the reported results.[21,31] The two absorption peaks at around 610 and 670 nm, which can be attributed to the characteristic A1 and B1 direct excitonic transitions of MoS_2 with the energy split from valence band spin–orbital coupling, indicate the existence of layered MoS_2 dispersed in the mixed solvent. Assuming that the dispersion obeys the Lambert–Beer law, the concentration of the dispersion was calculated to be 3.5 μg mL^{-1} by using the extinction coefficient (3400 mL mg^{-1} m^{-1} at 670 nm) reported in the literature.[31] The morphology and thickness of the MoS_2 nanosheets were characterized by AFM. As shown in Fig. S1,† the as-prepared MoS_2 had an average dimension of a few tens of nanometers and a height of around 2 nanometers, indicating that they are not single layered (thickness 0.65 nm) but stacked few layers.

Principle and feasibility of the Dam MTase activity assay

Early studies have reported that aromatic (*e.g.* pyridine, purine, *etc.*) and conjugated compounds can be physically absorbed on the basal plane of MoS_2 using either theoretical calculations or experimental studies.[32,33] Moreover, recent studies have revealed that layered 2D TMDCs, like MoS_2 and WS_2, could adsorb oligonucleotides *via* van der Waals interactions and could effectively quench the fluorescence of fluorophores labeled at the end of absorbed single-stranded DNA *via* energy transfer.[25–27] To adopt MoS_2 nanosheets as a fluorescence quencher for homogeneous detection of Dam MTase activity, Dam MTase/DpnI, which specifically methylates/cleaves the adenosine residues in the double-stranded 5′-GATC-3′ DNA sequence, was chosen as the MTase/endonuclease model. The substrate DNA consisted of a single-stranded region for MoS_2 absorption and a double-stranded region containing the Dam/DpnI recognition site, a FAM fluorescent dye was conjugated at the inner end of the duplex region. As illustrated in Fig. 2, the substrate DNA was successively treated with Dam and DpnI, methylated DNA was specifically cleaved by the methylation sensitive endonuclease DpnI. After cleavage, the remaining fluorophore conjugated 5-base segment was expected to be released as a result of the extremely low melting temperature of the 5-base pair duplex region. Upon the addition of MoS_2 nanosheets, fluorescence of non-methylated DNA was quenched due to the close contact of fluorophore and the MoS_2 nanosheets. However, the fluorescence of the short segment was retained because of its weak van der Waals interactions with MoS_2.

To avoid changing the buffer for different enzymatic reactions, the activities of Dam and DpnI were firstly evaluated in R buffer. The substrate DNA was successively treated with Dam and DpnI, and solely treated with Dam or DpnI for control as well. The gel image in Fig. 3a shows that there are two split bands in the Dam + DpnI treated sample (lane 4), the upper band at the same position with the controls (lane 1, lane 2, and lane 3) was the non-methylated substrate DNA, and the lower band was the cleaved DNA fragment (25 bases ss-DNA and 24 bases ds-DNA). The result indicated the successful methylation and cleavage reaction and thus the guaranteed activity of the two enzymes in R buffer. The melting tempera-

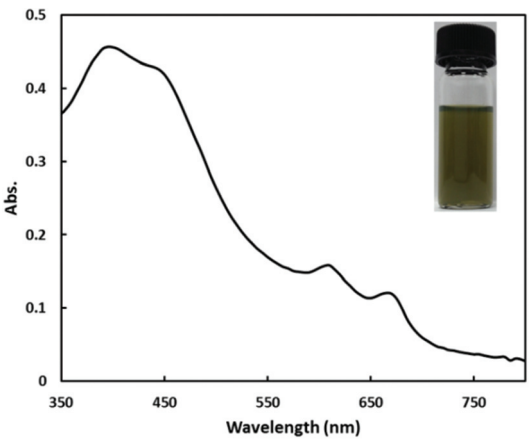

Fig. 1 UV-vis spectrum of as-prepared MoS_2 nanosheets. Inset: photograph of the MoS_2 suspension.

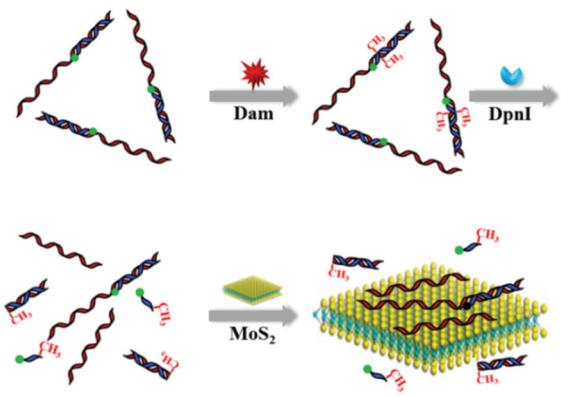

Fig. 2 Schematic illustration of the proposed fluorescence Dam MTase activity assay.

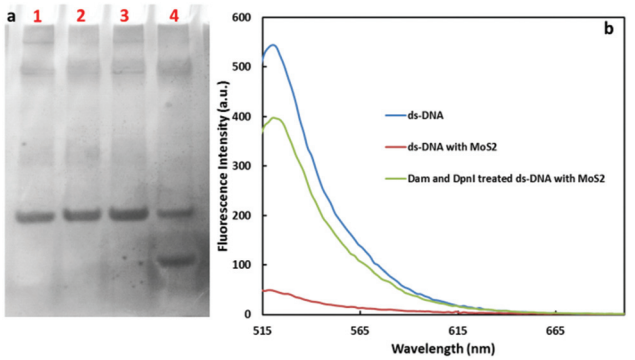

Fig. 3 (a) Gel image of 4 μM substrate DNA. Lane 1: ds-DNA, lane 2: Dam treated ds-DNA, lane 3: DpnI treated ds-DNA, and lane 4: Dam + DpnI treated ds-DNA. (b) Fluorescence emission spectra of substrate ds-DNA, substrate ds-DNA with the MoS_2 nanosheets, and Dam/DpnI treated substrate ds-DNA with the MoS_2 nanosheets. Excitation wavelength: 495 nm.

ture of the 5-base pair remaining duplex region is calculated to be less than 10 °C in R buffer, therefore the fluorophore labeled 5-base fragment readily dehybridizes and desorbs from the MoS_2 nanosheets after the DpnI cleavage. It was found that the fluorophore-labeled fragment having up to 10 bases readily desorbs from MoS_2 nanosheets after cleavage. Fig. 3b shows the fluorescence quenching–restoration behavior mediated by MoS_2 nanosheets. As can be seen, the fluorescence of the FAM-labeled substrate was almost fully quenched in the presence of the MoS_2 sheets (traces 1 and 2), whereas the fluorescence was turned on when the substrate DNA was treated with Dam and DpnI, as a result of the partially released fluorophores. In addition, to further understand the quenching mechanism, the fluorescence lifetime of the FAM labeled substrate DNA in the absence and in the prescence of the MoS_2 nanosheets were measured (Fig. S2†). In the prescence of the MoS_2 nanosheets, the fluorophore displayed faster decay than the free FAM-labeled substrate DNA, indicating that the quenching mechanism is dynamic, thus clearly confirming the feasibility of employing the MoS_2 nanosheets as an effective fluorescence quencher for the Dam activity assay.

Dam methyltransferase activity assay

To obtain sufficient quenching efficiency with a minimal amount of the MoS_2 nanosheets, the amount of the MoS_2 nanosheets was optimized (ESI† Fig. S3). It was found that the optimal concentration of the MoS_2 nanosheets in the final quenching system is 1.75 μg mL^{-1}. It is worth noting that under the experimental conditions, the MoS_2 nanosheets showed superior quenching efficiency when compared with graphene oxide sheets (Fig. S4†), which is likely attributed to its excellent energy harvesting property. Next, the time needed to reach the equilibrium upon the addition of the MoS_2 nanosheets was investigated as well. As shown in Fig. S5,† the quenching process is very fast. The fluorescence intensity decreased sharply in the first 20 s, and almost reached the equilibrium within 10 min. Thereafter, the DNA sample and the MoS_2 nanosheets mixture was allowed to stand for 10 min before fluorescence recording. It is worth mentioning that centrifugation could effectively reduce the background signal as depicted in Fig. S6.† This could be attributed to the possibility that the single-stranded region of some FAM-labeled substrate DNA was partially absorbed on MoS_2, the FAM fluorophore was a overhang outside the MoS_2 nanosheets, the fluorescence of FAM in such case could not be quenched effectively due to the long distance between the fluorophore (energy donor) and MoS_2 (energy acceptor). However, the partially absorbed substrate DNA could be separated from the solution together with MoS_2 under centrifugal force, which contributed to the low background signal.

Under the optimal experimental conditions, the performance of the developed assay for quantitative detection of Dam MTase activity was further examined. Fig. 4a displays the fluorescence emission spectra of the sensing system treated with different concentrations of Dam MTase, the fluorescence

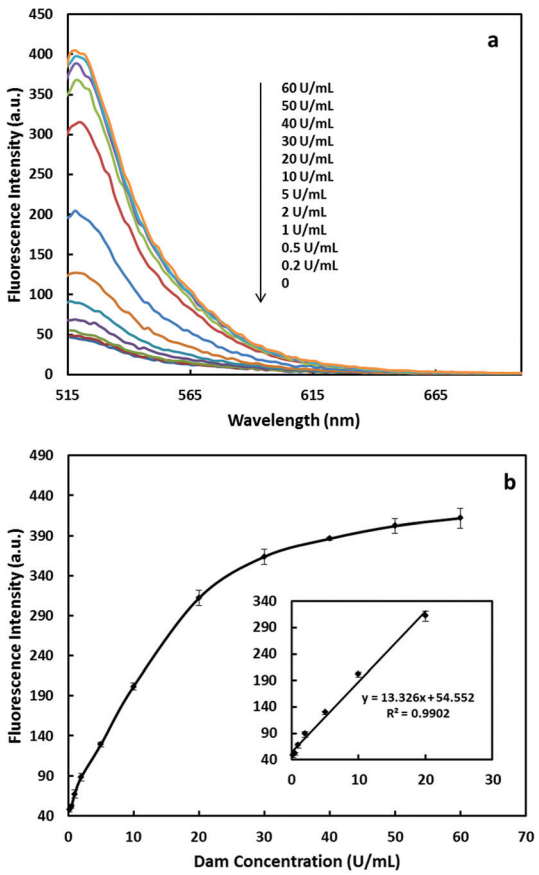

Fig. 4 (a) Fluorescence spectra of FAM-labeled substrate DNA treated with different concentrations of Dam MTase: 0 (control), 0.2, 0.5, 1, 2, 5, 10, 20, 30, 40, 50, 60 U mL^{-1}. Excitation wavelength: 495 nm. (b) The corresponding plot of fluorescence intensity *versus* the concentration of Dam MTase from 0 to 60 U mL^{-1}. Inset: linear correlation from 0.2 to 20 U mL^{-1}.

intensity increased rapidly as the Dam MTase concentration varied from 0 to 20 U mL^{-1}, and gradually levelled off beyond 20 U mL^{-1}. The corresponding calibration curve is plotted in Fig. 4b. The linear relationship between the fluorescence intensity at 518 nm and the Dam MTase concentration was observed from 0.2 to 20 U mL^{-1} with satisfactory sensitivity and a correlation coefficient (R^2) of 0.99. The detection limit was estimated to be 0.14 U mL^{-1} based on three times the standard deviation of the background fluorescence signal over the slope of the calibration curve. The performance of the proposed assay is comparable or even better than that of reported Dam MTase activity assays.[12,14]

Selectivity and inhibition study

The selectivity of the proposed Dam MTase activity assay was further investigated using AluI MTase and M.SssI MTase as the interference enzymes. Both AluI MTase and M.SssI MTase belong to the DNA cytosine methyltransferase family. AluI MTase specifically methylates the cytosine residue (C^5) of the sequence 5′-AGCT-3′ within the duplex DNA, and M.SssI modifies the cytosine residue (C^5) within the double-stranded dinucleotide recognition sequence 5′-CG-3′. As depicted in Fig. 5, both the fluorescence responses of the AluI MTase and M.SssI MTase treated substrate DNA were practically the same as the control. In contrast, significantly higher fluorescence intensity was obtained with the Dam MTase treated substrate DNA thus readily allowing highly selective detection of Dam MTase activity. Therefore, the proposed assay exhibits extraordinary selectivity and can easily discriminate Dam MTase from other interference enzymes owing to the highly specific sequence recognition of Dam MTase towards the substrate DNA.

Since Dam MTase is essential for bacterial virulence, Dam inhibitors are likely to have a broad antimicrobial action, and the investigation of Dam inhibition is of great importance for antimicrobial drug development.[34] 5-Fluorouracil, a well-known inhibitor of MTase which has been popularly used for cancer therapy for about 40 years,[35,36] was selected as the model Dam MTase inhibitor in this study. Fig. 6 shows that the relative activity of Dam MTase monotonically decreased with the increasing concentration of 5-fluorouracil in a dose-dependent manner. The IC_{50} (half maximal inhibitory concentration) value of 5-fluorouracil was calculated to be 17.7 μM. Hence, the proposed method is demonstrated to be a potentially useful tool for antimicrobial drug discovery.

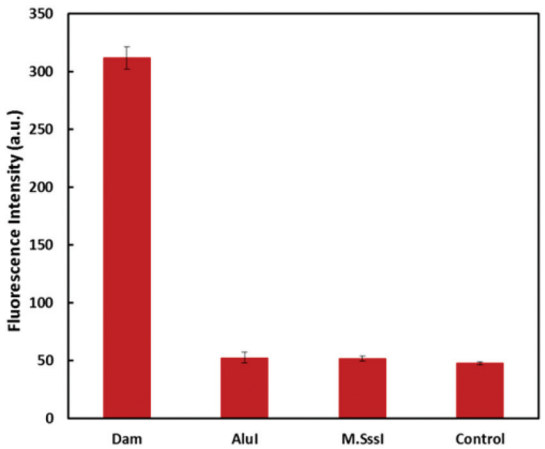

Fig. 5 Selectivity of the proposed Dam MTase activity towards interference enzymes of AluI MTase and M.SssI MTase. MTase concentration: 20 U mL^{-1}.

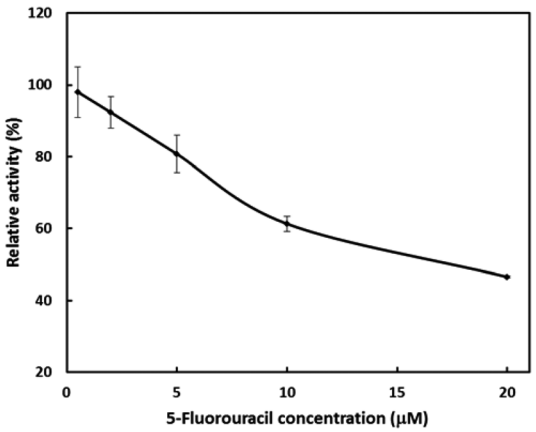

Fig. 6 Relative activity of Dam MTase inhibited with different concentrations of 5-fluorouracil.

Conclusions

In summary, a simple homogeneous fluorescence assay for the detection of Dam MTase activity by employing the MoS_2 nanosheets as the energy acceptor in fluorescence quenching has been developed. Good sensitivity and selectivity were observed. The fluorescence "turn on" strategy greatly improved the suitability of the assay in MTase activity assessments. The simplicity, high sensitivity, and the usage of newly emerging MoS_2 nanosheets are some of the interesting features for the development of a simple, robust, low cost, and highly sensitive MTase activity assay for uses in decentralized settings. In addition, the successful application of the MoS_2 nanosheets in MTase activity quantification not only made the biological applications of the newly emerging 2D IGAs a step further, but also provided a potentially useful platform for sensitive Dam MTase activity monitoring and for MTase inhibitor screening in biomedical research and clinical diagnosis.

Acknowledgements

The authors gratefully acknowledge financial support for this work from Ministry of Education and the A*STAR-ANR program.

Notes and references

1 X. D. Cheng and R. J. Roberts, *Nucleic Acids Res.*, 2001, **29**, 3784–3795.

2 W. Reik, W. Dean and J. Walter, *Science*, 2001, **293**, 1089–1093.
3 A. Razin and H. Cedar, *Microbiol. Rev.*, 1991, **55**, 451–458.
4 E. Li, C. Beard and R. Jaenisch, *Nature*, 1993, **366**, 362–365.
5 G. Csankovszki, A. Nagy and R. Jaenisch, *J. Cell Biol.*, 2001, **153**, 773–784.
6 K. Mutze, R. Langer, F. Schumacher, K. Becker, K. Ott, A. Novotny, A. Hapfelmeier, H. Höfler and G. Keller, *Eur. J. Cancer*, 2011, **47**, 1817–1825.
7 S. A. Belinsky, K. J. Nikula, S. B. Baylin and J. P. Issa, *Proc. Natl. Acad. Sci. U. S. A.*, 1996, **93**, 4045–4050.
8 A. Bergerat, W. Guschlbauer and G. V. Fazakerlry, *Proc. Natl. Acad. Sci. U. S. A.*, 1991, **88**, 6394–6397.
9 E. Boye, M. G. Marinus and A. Løbner-Olesen, *J. Bacteriol.*, 1993, **174**, 1682–1685.
10 J. G. Herman, J. R. Graff, S. Myöhänen, B. D. Nelkin and S. B. Baylin, *Proc. Natl. Acad. Sci. U. S. A.*, 1996, **93**, 9821–9826.
11 S. Friso, S. W. Choi, G. G. Dolnikowski and J. Selhub, *Anal. Chem.*, 2002, **174**, 4526–4531.
12 J. Li, H. F. Yan, K. M. Wang, W. H. Tan and X. W. Zhou, *Anal. Chem.*, 2007, **79**, 1050–1056.
13 J. Lee, Y. K. Kim and D. H. Min, *Anal. Chem.*, 2011, **83**, 8906–8912.
14 W. Li, Z. L. Liu, H. Lin, Z. Nie and J. H. Chen, *Anal. Chem.*, 2010, **82**, 1935–1941.
15 T. Liu, J. Zhao, D. M. Zhang and G. X. Li, *Anal. Chem.*, 2010, **82**, 229–233.
16 H. W. Wu, S. C. Liu, J. H. Jiang, G. L. Shen and R. Q. Yu, *Chem. Commun.*, 2012, **48**, 6280–6282.
17 H. M. Deng, X. J. Yang, S. P. X. Yeo and Z. Q. Gao, *Anal. Chem.*, 2014, **86**, 2117–2123.
18 X. Y. Ouyang, J. H. Liu, J. S. Li and R. H. Yang, *Chem. Commun.*, 2012, **48**, 88–90.
19 Y. H. Wang, X. X. He, K. M. Wang, J. Su, Z. F. Chen, G. P. Yan and Y. D. Du, *Biosens. Bioelectron.*, 2013, **41**, 238–243.
20 H. S. S. R. Matte, A. Gomathi, A. K. Manna, D. J. Late, R. Datta, S. K. Pati and C. N. Rao, *Angew. Chem., Int. Ed.*, 2010, **49**, 4059–4062.
21 J. N. Coleman, M. Lotya, A. O'Neill, S. D. Bergin, P. J. King, U. Khan, K. Young, A. Gaucher, S. De, R. J. Smith, I. V. Shvets, S. K. Arora, G. Stanton, H. Y. Kim, K. Lee, G. T. Kim, G. S. Duesberg, T. Hallam, J. J. Boland, J. J. Wang, J. F. Donegan, J. C. Grunlan, G. Moriarty, A. Shmeliov, R. J. Nicholls, J. M. Perkins, E. M. Grieveson, K. Theuwissen, D. W. McComb, P. D. Nellist and V. Nicolosi, *Science*, 2011, **331**, 568–571.
22 J. F. Xie, J. J. Zhang, S. Li, F. Grote, X. D. Zhang, H. Zhang, R. X. Wang, Y. Lei, B. C. Pan and Y. Xie, *J. Am. Chem. Soc.*, 2013, **135**, 17881–17888.
23 K. Chang and W. X. Chen, *ACS Nano*, 2011, **5**, 4720–4728.
24 K. Lee, R. Gatensby, N. McEcoy, T. Hallam and G. S. Duesberg, *Adv. Mater.*, 2013, **25**, 6699–6702.
25 C. F. Zhu, Z. Y. Zeng, H. Li, F. Li, C. H. Fan and H. Zhang, *J. Am. Chem. Soc.*, 2013, **135**, 5988–6001.
26 Q. Xi, D. M. Zhou, Y. Y. Kan, J. Ge, Z. K. Wu, R. Q. Yu and J. H. Jiang, *Anal. Chem.*, 2014, **86**, 1361–1365.
27 Y. X. Yuan, R. Q. Li and Z. H. Liu, *Anal. Chem.*, 2014, **86**, 3610–3615.
28 J. Z. Ou, A. F. Chrimes, Y. C. Wang, S. Y. Tang, M. S. Strano and K. Kalantar-zadeh, *Nano Lett.*, 2014, **14**, 857–863.
29 L. Wang, Y. Wang, J. I. Wong, T. Palacios, J. Kong and H. Y. Yang, *Small*, 2014, **10**, 1101–1105.
30 H. Y. Song, Y. N. Ni and S. Kokot, *Biosens. Bioelectron.*, 2014, **56**, 137–143.
31 K. G. Zhou, N. N. Mao, H. X. Wang, Y. Peng and H. L. Zhang, *Angew. Chem., Int. Ed.*, 2011, **50**, 10839–10842.
32 P. G. Moses, J. J. Mortensen, B. I. Lundqvist and J. K. Norskov, *J. Chem. Phys.*, 2009, **130**, 104709.
33 W. M. Heckl, D. P. E. Smith, G. Binnig, H. Klagges, T. W. Hänsch and J. Maddocks, *Proc. Natl. Acad. Sci. U. S. A.*, 1991, **88**, 8003–8005.
34 D. M. Heithoff, R. L. Sinsheimer, D. A. Low and M. J. Mahan, *Science*, 1999, **284**, 967–970.
35 C. G. Moertel, S. Frytak, R. G. Hahn, M. J. O'Connell, R. J. Reitemeier, J. Rubin, A. J. Schutt, L. H. Weiland, D. S. Childs, M. A. Holbrook, P. T. Lavin, E. Livstone, H. Spiro, A. Knowlton, M. Kalser, J. Barkin, H. Lessner, R. Mann-Kaplan, K. Ramming, H. O. Douglas Jr., P. Thomas, H. Nave, J. Bateman, J. Lokich, J. Brooks, J. Chaffey, J. M. Corson, N. Zamcheck and J. W. Novak, *Cancer*, 1981, **48**, 1705–1710.
36 D. Salonga, K. D. Danenberg, M. Johnson, R. Metzger, S. Groshen, D. D. Tsao-Wei, H. J. Lenz, C. G. Leichman, L. Leichman, R. B. Diasio and P. V. Danenberg, *Clin. Cancer Res.*, 2000, **6**, 1322–1327.